The Use of Quantum Dots for Analysis of Chick CAM Vasculature

Jason D. Smith[†§], Gregory W. Fisher[§], Alan S. Waggoner[§], and Phil G. Campbell[†§*]

[†]Institute for Complex Engineered Systems, Carnegie Mellon University, 5000 Forbes Ave., Pittsburgh, PA 15213, [§]Molecular Biosensor and Imaging Center Carnegie Mellon University, 4400 Fifth Ave., Pittsburgh, PA 15213

*Correspondence should be addressed to:

Phil Campbell, Ph.D.
1212 Hamburg Hall
Institute for Complex Engineered Systems
Carnegie Mellon University
5000 Forbes Ave
Pittsburgh, PA, PA 15213
Phone: (412) 268-4126
Fax: (412) 268-5229
Email: pcampbel@cs.cmu.edu

ABSTRACT

Quantum dots (QDs) are fluorescent semiconductor nanocrystals that possess a number of superior fluorescent properties compared to more established organic dyes and fluorescent proteins. As a result, QDs are being studied for use in a wide range of biological applications. We have examined QDs for one such application, visualization of blood vessels of the chick chorioallantoic membrane (CAM), a popular model for studying various aspects of blood vessel development including angiogenesis. Intravitally injected QDs were found to be biocompatible and were kept in circulation over the course of four days without any observed deleterious effects. QD vascular residence time was tunable through QD surface chemistry modification. We also found that use of QDs with higher emission wavelengths (> 655 nm) virtually eliminated all chick-derived autofluorescence and improved depth-of-field imaging. QDs were compared to FITC-Dextrans, a fluorescent dye commonly used for imaging CAM vessels. QDs were found to image vessels as well as or better than FITC-Dextrans at 2-3 orders of magnitude lower concentration. We also demonstrated that QDs are fixable with low fluorescence loss and thus can be used in conjunction with histological processing for further sample analysis.

Keywords: Quantum Dots; FITC-Dextran; Chick CAM; Blood Vessels; Microscopy; Fluorescence

INTRODUCTION

Blood vessel development and formation is a widely researched area, due in part to the realization that tumors recruit new blood vessels from the host for growth and metastasis (Folkman, 1971; Folkman, 1990; Weidner et al., 1991). Intravital injection of fluorescent molecules is a desirable method for studying blood vessels due to its minimal-invasive nature. Using this method, numerous studies have investigated blood vessel development and function under normal and pathological conditions. For example, intravital injection of fluorescent molecules has been used to study properties of microcirculation in rats (Minamitani et al., 2003), brain blood flow in live, awake mice (Helmchen et al., 2001), vessel permeability and barrier function in the chick chorioallantoic membrane (CAM) (Cruz et al., 2000; Cruz et al., 1997; DeFouw and DeFouw, 2000a; DeFouw and DeFouw, 2000b; Rizzo and DeFouw, 1996; Rizzo et al., 1995; Rizzo et al., 1993), small ovarian metastases in the abdominal cavity of human subjects (Aalders et al., 2004), and 3D image reconstructions of tumor-associated vasculature (Tozer et al., 2005).

Quantum dots (QDs), which are fluorescent semiconductor nanocrystals (Watson et al., 2003), have exploded onto the biology scene, largely within the last few years (Michalet et al., 2005). QDs have a number of advantages over most organic dyes: they are highly resistant to photobleaching, possess broad excitation bands, have high molar absorptivities, large Stokes shifts, narrow fluorescence emission bands, and they can emit at a wide variety of wavelengths (Watson et al., 2003).

QDs have proven to be quite versatile as fluorescent probes, most notably due to their ability to be functionalized. *In vitro*, functionalized QDs have been used for protein/cell labeling and detection as well as for the investigation of cellular trafficking and signal transduction (Bruchez et al., 1998; Chan and Nie, 1998; Colton et al., 2004; Hasegawa et al., 2005; Hoshino et al., 2004; Howarth et al., 2005; Lidke et al., 2004; Rosenthal et al., 2002; Tomlinson et al., 2005; Wu et al., 2003). *In vivo*, Rieger et al. employed QDs as labeling agents for studying tissues in zebrafish embryos (Rieger et al., 2005), and Akerman et al. showed that intravitally injected ligand-coated QDs could specifically target organs and tumors in mice (Akerman et al., 2002). Non-invasive imaging of mouse tumors and organs, including vasculature, has also been demonstrated (Ballou et al., 2005; Ballou et al., 2004; Gao et al., 2004; Kim et al., 2004; Morgan et al., 2005). Similarly, QDs were used to perform sentinel lymph node mapping by image guidance alone in mice, rats, and pigs (Kim et al., 2004; Parungo et al., 2005; Soltesz et al., 2006).

We now extend the use of QDs into chick CAM blood vessel imaging. First used over 50 years ago, the CAM assay has become a mainstay of *in vivo* angiogenesis assays (Auerbach et al., 2003) and a model test system for blood vessel formation and development (Cruz et al., 2000; Cruz et al., 1997; DeFouw and DeFouw, 2000a; DeFouw and DeFouw, 2000b; Djonov et al., 2000a; Djonov et al., 2000b; Rizzo and DeFouw, 1996; Rizzo et al., 1995; Rizzo et al., 1993). Additionally, the CAM assay has been used to test the biocompatibility of biomaterials (Spanel-Borowski, 1989; Valdes et al., 2003; Valdes et al., 2002) and the angiogenic nature of tissue engineered constructs (Borges et al., 2003a; Borges et al., 2003b; Rickert et al., 2003).

In the present work we examine that QDs are an ideal fluorescence tool for imaging CAM vessels both *in situ* and post-histological processing. We demonstrate that QDs are biocompatible in the chick embryo and that they image CAM vasculature as well or better than FITC-Dextrans, a fluorescent molecule commonly used for CAM vessel imaging. QDs also demonstrated reduced interference from chick-derived autofluorescence, allowed for improved depth-of-field imaging, and were fixable in both glutaraldehyde and paraformaldehyde, thus making them valuable for fluorescence visualization post-histological processing.

MATERIALS AND METHODS

Materials

White Leghorn eggs were purchased from a local farm and incubated at 38ºC and 70% humidity (G.Q.F. Manufacturing Co., Savannah, GA). On day three, eggs were cracked into Petri dishes containing 4 mL Dulbecco's Modified Eagles Medium (Gibco, Carlsbad, CA) and incubated at 37ºC. As is typically performed in the literature, FITC-Dextran molecules (Sigma, St. Louis, MO) were prepared as 5% solutions: 98 μM 500 kD, 357 μM 150 kD, 850 μM 70 kD, 1200 μM 40 kD, and 2860 μM 20 kD FITC-Dextran. Multiple types of QDs were generously provided by Quantum Dot Corporation (Hayward, CA): 565 nm emission QDs conjugated with polyethylene glycol (PEG) and streptavidin (565PEG-SAv); 585PEG-SAv; 605PEG-SAv; non-conjugated, amphiphilic (AMP) polyacrylic acid-coated 655 nm emission QDs (655AMP); 705 nm emission QDs conjugated with long-chain (2000 Da) amino-PEG (705PEGa); 705AMP; 755PEGa; and long-chain (5000 Da) methoxy-PEG 800 nm emission QDs (800PEGm). QDs were

formulated in the range of 1-4 μM. Human fibrinogen (gift of ZLB Behring, King of Prussia, PA), human thrombin (Enzyme Research Labs, South Bend, IN), and recombinant human fibroblast growth factor-2 (FGF-2) (PeproTech Inc., Rocky Hill, NJ) were buffered in 20 mM HEPES, 150 mM NaCl, pH 7.4. Glutaraldehyde and paraformaldehyde, 25% and 16% in solution, respectively, were purchased from Electron Microscopy Sciences (Hatfield, PA).

Fibrin Gel Formation

Human fibrinogen was mixed with recombinant bovine aprotinin (Sigma) and FGF-2 to a final concentration of 13.6 mg/mL fibrinogen, 1 μg/mL aprotinin, and 10 ng/mL FGF-2. The fibrinogen mixture (55 μL) was added to 4 μL of 100 U/mL human thrombin and 55 μL of the mixture was immediately transferred to an 8 mm diameter X 1 mm tall mold and allowed to gel. Fibrin disks were removed from the mold and placed on the CAM of 10-day old chick embryos. After 2 days on the CAM QD:FITC-Dextran mixtures were injected and angiogenic responses imaged. For QD-labeled fibrinogen experiments, a fibrinogen solution with the following final concentrations was prepared: 18 mg/mL fibrinogen, 1 mg/mL biotinylated fibrinogen, 1 μg/mL aprotinin, 15 nM 605PEG-SAv QDs conjugated with streptavidin, and 10 ng/mL FGF-2 in 20 mM HEPES, 100 mM NaCl, pH 7.4. Gels were formed in the same manner as above.

Injections

QDs were sonicated for 10 minutes and mixed with an equal volume of FITC-Dextrans. A concentrated saline solution was added to the QD:FITC-Dextran solution to 154 mM

NaCl prior to injection. Superficial CAM veins were injected with 20-25 μL of the QD:FITC-Dextran mixture using an aspirator tube assembly (Sigma) and borosilicate capillaries (Sutter Instruments, Novato, CA), which were pulled into micro-needles using a Model P-87 micropipette puller (Sutter Instruments).

Chick CAM Microscopy

For each embryo images were taken of a large CAM vein over time with a M2BIO (Kramer Scientific, Valley Cottage, NY) stereomicroscope using a 1.6X objective (0.075 NA) at 1X zoom, a Star/O 1 Watt blue laser diode (Luxeon, San Jose, CA) excitation source, and a Retiga Exi cooled CCD camera (QImaging, Burnaby, BC, Canada). FITC-Dextran fluorescence was imaged using a 450 nm excitation-546/30 nm emission filter set (Chroma, Rockingham, VT) and QD fluorescence was imaged with a 450 nm excitation-500 nm long pass emission (Chroma) or 450 nm excitation-660 nm long pass emission filter set (Chroma). Images involving 800 nm-emitting QDs were acquired using an Orca II cooled CCD camera (Hamamatsu, Bridgewater, NJ) and 820/40 nm filter (Chroma). Acquisition times for fluorescence half-life experiments for FITC-Dextrans and QDs were 60 seconds and 20 seconds, respectively. Capillaries were imaged on the M2BIO stereomicroscope using a 10X objective (0.45 NA) at 4X zoom. Acquisition times for capillary imaging FITC-Dextrans and QDs were 3 seconds and 1 second, respectively. Angiogenic responses to fibrin-based tissue engineered constructs were imaged using the M2BIO microscope with the above filter sets. Image acquisition times were approximately 10 and 30 seconds for QDs and FITC-Dextrans, respectively.

Images for QD fixation studies were acquired using the M2BIO stereomicroscope with a 1.6X objective at 0.8X zoom, a Star/O 1 Watt blue laser diode excitation source, and a Retiga Exi cooled CCD camera. For 605PEG-SAv, 655PEG-SAv, and 705PEG-SAv QDs the following filter sets were used: (Ex:Em) 450spuv:500LP; 450spuv:605/20; and 450spuv:705/20, respectively (Chroma).

Image Analysis

Illumination across images was normalized by flatfield dividing a background image of the light source. For time series experiments all images in a time series were scaled the same. Vascular fluorescence intensities of the scaled images were measured using Image J software v1.29 (NIH, Bethesda, MD). Multiple measurements were acquired for each sample, and from these values an average intensity was calculated. For time course experiments, average intensities over the course of the experiment were fitted to a least-squares exponential decay curve and half-life values were derived from the fit. Reported half-lives represent the average and SEM derived from at least three independent experiments except for the 20kD, 40kD, and 70kD FITC-Dextran experiments, which produced only 2, 1, and 2 data sets, respectively that could be fit with simple exponential decay.

Paraffin Histology

Approximately 200 μL of paraformaldehyde (0.5% in calcium-magnesium free PBS (CMF-PBS)) was pipetted directly onto the fibrin construct while on the CAM and incubated at room temperature for 5-10 minutes. The fibrin and connected CAM were excised and stored in 1% paraformaldehyde at 4°C overnight. The sample was then sent to a local laboratory (Consultants in Veterinary Pathology, Inc., Murrysville, PA) where it was processed for embedding in paraffin and sectioned at 5 μm on a rotary microtome. QD fluorescence images of sections were obtained using a Zeiss Axioplan epifluorescence microscope with a 10X objective (0.3 NA) and the Retiga Exi CCD

camera. Filter sets for 605 and 705 nm emitting QDs were (Ex:Em) 450spuv:610/40 and 450spuv:700LP, respectively (Chroma).

RESULTS

To demonstrate the utility of QDs in visualizing chick CAM vasculature, a series of QDs were intravitally injected into individual 10-day old chick embryos and CAM vessels were imaged (Figure 1). Vessels injected with short wavelength-emitting QDs (< 655 nm) appeared dim due to autofluorescence from the allantoic sac and absorbance of QD fluorescence by hemoglobin (Figure 1A, B). Vessel visualization improved with the use of 605 nm emitting QDs and became devoid of interference at wavelengths greater than 655 nm (Figures 1D-F). Importantly, all QDs tested were found to be biocompatible, and chick viability and development appeared unaffected during time-course experiments involving multiple QD injections (data not shown).

Additional images of chick CAM vasculature are shown in Figure 2. The entire chick embryo vasculature was imaged with intravitally injected 755PEGa QDs (Figure 2A). Because there was no autofluorescence with 755 nm emitting QDs, the CAM and underlying yolk vessels (Figure 2B) could be co-imaged. However, QDs were lost from the vessel lumen over time. Interestingly, low-level fluorescence was clearly retained within vessel walls ranging from veins to capillaries (Figure 2C), although it was not of a sufficient level to obtain high quality, low magnification images of the CAM vasculature. QD retention was most likely due to QD endocytosis and storage within lysosomes rather than the result of specific endothelial cell targeting (Hanaki et al., 2003).

QDs were then compared to FITC-Dextrans, a dye commonly used for CAM vessel imaging. 705 nm-emission QDs were chosen for these experiments because of the low autofluorescence signal at this wavelength. 705PEGa QDs were co-injected with FITC-Dextran molecules, and fluorescent images of CAM vessels were taken over time (Figures 3, 4). Initial images post-injection demonstrate that 705PEGa QDs and high molecular weight FITC-Dextrans (150 kD or 500 kD) comparably imaged CAM vasculature (Figure 3A, B; Figure 4A, B). However, QD concentrations used were approximately 100 and 30 times less than the 150 kD and 500 kD FITC-Dextrans concentrations, respectively. This is due in part to the QD's approximately 10-fold higher molar absorptivity compared to fluorescein (Watson et al., 2003). Lower molecular weight FITC-Dextrans (20 and 40 kD) were difficult to directly compare to 705PEGa QDs because their vascular residence times were quite short. This led to low vessel fluorescence and high background levels in the surrounding space (Figure 3F, H).

As a further comparison, half-lives of FITC-Dextrans and QDs in the CAM vasculature were calculated (Table 1). Fluorescence data was fit to single exponential decay curves from which the decay constants were used to calculate half-lives. FITC-Dextran half-lives decreased with decreasing molecular weight, a function of the size-dependence on extravasation from the capillaries. 705PEGa QDs had approximately twice the half-life of 705AMP QDs, demonstrating that QD functionalization can modulate vasculature retention times. Although their half-lives were similar, vessel image quality from the 705PEGa QDs and 500 kD FITC-Dextran was strikingly different (Table 1, Figure 4). Unlike the QDs tested, 500kD FITC-Dextran, as well as every other

FITC-Dextran tested, accumulated over time in the allantoic sac, significantly increasing background fluorescence (Figure 4D, also seen in Figure 3F).

Because FITC-Dextrans and QDs visualize larger CAM vasculature in a comparable manner, we also wanted to examine their ability to visualize CAM capillary structure. The capillaries and pre- and post-capillary vessels were imaged comparably with both FITC-Dextrans and QDs (Figure 5). As was the case with the previous imaging experiments (Figures 3, 4), injected QD levels were approximately two orders of magnitude lower than the FITC-Dextrans.

For tissue engineering applications we compared the abilities of FITC-Dextrans and QDs to image CAM blood vessel responses to fibrin-based tissue engineered constructs containing FGF-2, a commonly used angiogenic factor (Bikfalvi et al., 1997; Ribatti et al., 1997; Wong et al., 2003). Approximately 2 days post-placement of the gel on the CAM, 150kD or 500kD FITC-Dextrans were co-injected with 705PEGa or 800PEGm QDs and the angiogenic responses were imaged (Figure 6). The blood vessel response, hallmarked by the spoke-wheel vessel pattern around the fibrin matrix, was comparably imaged with the FITC-Dextrans and 705PEGa QDs. However, the QDs had higher emission wavelengths and thus improved the visualization of blood vessels underlying the fibrin construct (comparison of Figure 6C, E, and G to Figure 6D, F, and H).

The fibrin constructs were initially clear but became more optically dense as they were contracted, remodeled, and degraded by the responding CAM tissue (as seen in Figure 6). Although the higher emission QDs allowed for improved depth of field, it was not always possible to visualize vessels underlying the fibrin (Figure 6A, B). Given this,

we also used histology-based techniques to examine the CAM response. Typically, samples would be paraffin-embedded, sectioned, and individually stained for blood vessel markers, a process that is time consuming, has inherent artifact problems, and results in section-to-section variability. We set out to investigate whether QDs could be applied pre-histological processing and still retain fluorescence post-processing.

We first investigated the ability of QDs to retain fluorescence post-fixation *in vitro*. Streptavidin conjugated QDs pre-bound to biotinylated fibrinogen were used to form fibrin gels that were then treated with fixatives. We tested 605, 655, and 705 nm emitting QDs. Fibrin gels were incubated in either 1% paraformaldehyde or 1% glutaraldehyde for 30 minutes followed by three 5 minute washes with PBS. Intensities of initial and post-fixation fluorescence images were quantitated by densitometry: fluorescence loss was not found to be statistically significant (Figure 7). Fibrin gels containing 605PEG-SAv QDs gained fluorescence during glutaraldehyde fixation, but this gain appeared to be due entirely to glutaraldehyde-induced fibrin autofluorescence (Figure 7A). This was not seen with the other two QDs, because there is lower fixative-induced autofluorescence at these wavelengths and because of the short bandpass of the emission filters used.

We also examined the effects of longer-term glutaraldehyde and paraformaldehyde fixation. 655PEG-SAv QD fluorescence in biotinylated fibrin gels was followed over time in both 1% glutaraldehyde and 1% paraformaldehyde. After approximately 48 hours, the fibrin-containing QDs in 1% glutaraldehyde lost 50% of their fluorescence intensity while those in 1% paraformaldehyde essentially did not lose their intensity (data not shown). Higher levels of fixatives (1% glutaraldehyde and 3%

paraformaldehyde) were employed for samples that were further examined by electron microscopy (submitted manuscript). QD fluorescence retention was not measured in these cases but intense fluorescence still observed pre-histological processing.

QD fluorescence retention was then tested in an *in vivo* setting in the chick CAM assay. Fibrin gels containing FGF-2 and biotinylated fibrinogen pre-bound with 605PEG-SAv QDs were placed on the CAM of 10-day old embryos. After 48 hours, the CAM was intravitally injected with 705PEG QDs. The fibrin and connected CAM were excised, fixed in 1% paraformaldehyde overnight, paraffin embedded, and sectioned to 5 μm thickness. QD fluorescence was imaged in the area of the CAM/fibrin interface (Figure 8). QD-labeled fibrin fluorescence at the interface appeared as streaks (Figure 8A). On either side of the interface, small spherical globules of QD-labeled fibrin fluorescence were seen. These two fluorescence patterns (globules and streaks) most likely represented fibrin remodeling and degradation products initiated by the invasive CAM.

Intravitally injected QDs show blood vessels primarily in the plane of the image and perpendicular to the fibrin/CAM interface (Figure 8B), probably due to the chemotactic effect of FGF-2 released from the degrading fibrin. The few visible vessel lumens were mostly devoid of QDs (Figure 8B, arrows). Loss of luminal QDs from vessels was consistently seen during histological processing. Strong labeling of the vessel lining most likely represented uptake within endothelial cells.

To investigate the use of QDs in electron microscopy applications, we also fixed fibrin containing 655PEG-SAv QDs with osmium and examined fluorescence retention after treatment. Incubation with a concentration of 0.5% osmium for as little as 30

minutes completely destroyed all QD fluorescence (data not shown). However, samples not fixed in osmium and prepared in LR White plastic still retained QD fluorescence (data not shown).

DISCUSSION

In this work we have demonstrated the utility of QDs to image chick CAM vasculature. QDs with a range of emission wavelengths were injected and examined for their ability to optimally image CAM vasculature. QDs were also compared to FITC-Dextrans, fluorescent dyes commonly used in imaging chick CAM vasculature and angiogenic responses to fibrin-based tissue engineered constructs. Additionally, we also investigated the ability of QDs to be fixed and imaged post-processing.

Intravitally injected QDs imaged CAM vessels and capillaries with equal to superior ability compared to FITC-Dextrans. QDs were brighter, showed more equal illumination across vessel lumens, and had longer residence times, and could be used at much lower concentrations (Figures 3-6, Table 1). FITC-Dextran fluorescence measured in these experiments was not optimal. This is due to the fixed excitation wavelength (blue LED at 450 nm) and non-optimal emission filter to reduce spectral overlap. Therefore, actual FITC fluorescence intensity would more directly comparable to QD intensities. However, FITC-Dextrans accumulated in the allantoic sac over time, which increased background fluorescence levels (Figure 3, 4). This was not observed for comparable QD experiments, but it has been witnessed for QDs to a lesser degree in four-day CAM experiments involving multiple daily QD injections (data not shown).

Half-lives were similar for the 500kD and 150kD FITC-Dextrans but began to drop off dramatically around the 70kD FITC-Dextran down to the 40kD and 20kD FITC-Dextrans (Table 1). This behavior is indicative of selectivity in extravasation of molecules from the CAM capillaries. A cut-off around 70kD is a higher estimate than that determined in previous experiments (Cruz et al., 1997; Rizzo et al., 1995). A discrepancy is not unexpected, however, since our values are only inferred through fluorescence decay in large vessels and not directly measured. Due to the low number of usable samples, the 20, 40, and 70kD data should be taken with caution and primarily serves to show that these molecules are not useful for imaging CAM vessels over longer time periods.

QDs also demonstrated more uniform illumination across vessels, a property that may improve vessel identification and quantitation in various quantitative applications. Functionalization of QDs was also shown to tailor vascular residence time (Table 1). This study demonstrated that QDs are ideal intravital fluorescent molecules for noninvasive vessel imaging, especially for studies involving imaging over time.

Low emitting QDs (< 655 nm) were not effective for imaging CAM vessels (Figure 1). Interestingly, QD emission wavelengths used in Figure 1A-C (565, 585, and 605 nm) were higher than the emission wavelength of FITC (520 nm) although the QDs produced inferior images. This may be due to a sharp rise in hemoglobin adsorption from approximately 500-580 nm (Takatani and Graham, 1979). Additionally, unlike the 546/30 nm filter used for FITC-Dextrans, images for 565, 585, and 605 nm emitting QDs were acquired using a 500 nm long pass filter, which allowed more autofluorescence wavelengths to be collected. This most likely resulted in increased background

fluorescence levels and contributed to the poor vascular image quality for QD images. High emitting QDs (> 655 nm) virtually eliminated all chick-derived autofluorescence.

In addition to decreasing chick autofluorescence, increased emission wavelength also improved depth-of-field (Figure 1, Figure 6). Compared to FITC-Dextrans, higher wavelength-emitting QDs better imaged blood vessels underneath and within the fibrin (Figure 6). The development of near-IR QDs with higher emission wavelengths (800-950 nm) should further improve depth-of-field and vessel visualization. This opens doors for non-invasive imaging techniques involving the quantitation and/or 3D modeling of blood vessels in optically dense biomaterials in the CAM assay. Three dimensional image stacks could be obtained over time to create "angiogenic profiles" that could be used to design better tissue engineered constructs.

We also found that QDs can retain fluorescence after treatment with certain fixatives. Treatment of QDs with glutaraldehyde and paraformaldehyde over time showed glutaraldehyde to be more deleterious than paraformaldehyde to QD fluorescence (data not shown). Additionally, osmium treatment completely destroyed QD fluorescence. The mechanism by which fixatives destroy QD fluorescence is not known, but it probably involves their chemical effects on the amphiphilic molecular coating of the QDs. This coating protects the QD nanocrystal core from fluorescence-quenching water molecules. However, QDs prepared by other manufacturers utilizing different surface chemistries were not tested. It is possible that these other chemistries may better protect the core from penetration by water and thus improve QD fixability.

Overall, the general fixability of QDs allows for labeling pre-histological processing, which should shorten analysis time and reduce section-to-section variability

compared to labeling each section post-histological processing. Because osmium treatment destroys QD fluorescence, their use as fluorescent reporters in samples prepared for electron microscopy analysis is limited. However, QDs can still be identified by electron microscopy because they are electron-dense materials (Figure 9). In Figure 9 QDs are endocytosed and seen as electron-dense particles within endothelial cell vesicles.

During histological processing we did observe significant lumenal QD loss due to poor fixation of the blood, specifically in the graded ethanol dehydration steps. We tried two methods to retain higher QD levels. For better fixation of luminal contents and thus improved QD retention we experimented with co-intravital injection of warm 10% gelatin solution containing QDs. As the gelatin cooled and formed a gel a more "fixable" matrix formed. This process demonstrated improved QD retention upon fixation but was technically challenging to perform (data not shown). We also labeled streptavidin QDs with biotinylated Lens *culinaris agglutinin*, a lectin shown to label chick CAM vasculature, and injected them. Due to the high valency of biotin binding sites on the QD, it was difficult to control the number of lectins per QD. Experiments often resulted in aggregation of the QDs and localization primarily in capillary structures (data not shown).

Overall, QDs have shown to be excellent intravital fluorescent probes for imaging CAM blood vessels. They are extremely bright, are photostable, have low background interference, and shown an improved depth-of-imaging over FITC-Dextrans. By functionalizing QDs one can tailor vascular residence time and allow for target-based

detection. We have shown QDs retain fluorescence in paraffin-based histological analysis.

ACKNOWLEDGEMENTS

This work was supported by the NSF (CTS-0210238) and NIH (1 R01 EB00 364-01 and 1 T32 EB00424-03). Thanks to Lee Weiss (The Robotics Institute, Carnegie Mellon University) for helpful discussions and critical review of the manuscript. We also thank Aventis Behring LLC (King of Prussia, PA) and Quantum Dot Corporation (Marcel Bruchez, Hayward, CA) for their generous gifts of human thrombin and quantum dots, respectively.

REFERENCES

Aalders, M.C., Sterenborg, D.J., Vange, N., 2004. Fluorescein angiography for the detection of metastases of ovarian tumor in the abdominal cavity, a feasibility pilot. Lasers Surg. Med. 35, 349-53.

Akerman, M.E., Chan, W.C., Laakkonen, P., Bhatia, S.N., Ruoslahti, E., 2002. Nanocrystal targeting in vivo. Proc. Natl. Acad. Sci. U S A 99, 12617-21.

Auerbach, R., Lewis, R., Shinners, B., Kubai, L., Akhtar, N., 2003. Angiogenesis assays: a critical overview. Clin. Chem. 49, 32-40.

Ballou, B., Ernst, L.A., Waggoner, A.S., 2005. Fluorescence imaging of tumors in vivo. Curr. Med. Chem. 12, 795-805.

Ballou, B., Lagerholm, B.C., Ernst, L.A., Bruchez, M.P., Waggoner, A.S., 2004. Noninvasive imaging of quantum dots in mice. Bioconjug. Chem. 15, 79-86.

Bikfalvi, A., Klein, S., Pintucci, G., Rifkin, D.B., 1997. Biological roles of fibroblast growth factor-2. Endocr. Rev. 18, 26-45.

Borges, J., Mueller, M.C., Padron, N.T., Tegtmeier, F., Lang, E.M., Stark, G.B., 2003a. Engineered adipose tissue supplied by functional microvessels. Tissue Eng. 9, 1263-70.

Borges, J., Tegtmeier, F.T., Padron, N.T., Mueller, M.C., Lang, E.M., Stark, G.B., 2003b. Chorioallantoic membrane angiogenesis model for tissue engineering: a new twist on a classic model. Tissue Eng. 9, 441-50.

Bruchez, M., Jr., Moronne, M., Gin, P., Weiss, S., Alivisatos, A.P., 1998. Semiconductor nanocrystals as fluorescent biological labels. Science 281, 2013-6.

Chan, W.C., Nie, S., 1998. Quantum dot bioconjugates for ultrasensitive nonisotopic detection. Science 281, 2016-8.

Colton, H.M., Falls, J.G., Ni, H., Kwanyuen, P., Creech, D., McNeil, E., Casey, W.M., Hamilton, G., Cariello, N.F., 2004. Visualization and quantitation of peroxisomes using fluorescent nanocrystals: treatment of rats and monkeys with fibrates and detection in the liver. Toxicol. Sci. 80, 183-92.

Cruz, A., DeFouw, L.M., DeFouw, D.O., 2000. Restrictive endothelial barrier function during normal angiogenesis in vivo: partial dependence on tyrosine dephosphorylation of beta-catenin. Microvasc. Res. 59, 195-203.

Cruz, A., Rizzo, V., De Fouw, D.O., 1997. Microvessels of the chick chorioallantoic membrane uniformly restrict albumin extravasation during angiogenesis and endothelial cytodifferentiation. Tissue Cell 29, 277-81.

DeFouw, L.M., DeFouw, D.O., 2000a. Differentiation of endothelial barrier function during normal angiogenesis requires homotypic VE-cadherin adhesion. Tissue Cell 32, 238-42.

DeFouw, L.M., DeFouw, D.O., 2000b. Vascular endothelial growth factor fails to acutely modulate endothelial permeability during early angiogenesis in the chick chorioallantoic membrane. Microvasc. Res. 60, 212-21.

Djonov, V., Schmid, M., Tschanz, S.A., Burri, P.H., 2000a. Intussusceptive angiogenesis: its role in embryonic vascular network formation. Circ. Res. 86, 286-92.

Djonov, V.G., Galli, A.B., Burri, P.H., 2000b. Intussusceptive arborization contributes to vascular tree formation in the chick chorio-allantoic membrane. Anat. Embryol. (Berl.) 202, 347-57.

Folkman, J., 1971. Tumor angiogenesis: therapeutic implications. N. Engl. J. Med. 285, 1182-6.

Folkman, J., 1990. What is the evidence that tumors are angiogenesis dependent? J. Natl. Cancer Inst. 82, 4-6.

Gao, X., Cui, Y., Levenson, R.M., Chung, L.W., Nie, S., 2004. In vivo cancer targeting and imaging with semiconductor quantum dots. Nat. Biotechnol. 22, 969-76.

Hanaki, K., Momo, A., Oku, T., Komoto, A., Maenosono, S., Yamaguchi, Y., Yamamoto, K., 2003. Semiconductor quantum dot/albumin complex is a long-life and highly photostable endosome marker. Biochem. Biophys. Res. Commun. 302, 496-501.

Hasegawa, U., Nomura, S.M., Kaul, S.C., Hirano, T., Akiyoshi, K., 2005. Nanogel-quantum dot hybrid nanoparticles for live cell imaging. Biochem. Biophys. Res. Commun. 331, 917-21.

Helmchen, F., Fee, M.S., Tank, D.W., Denk, W., 2001. A miniature head-mounted two-photon microscope. high-resolution brain imaging in freely moving animals. Neuron 31, 903-12.

Hoshino, A., Fujioka, K., Oku, T., Nakamura, S., Suga, M., Yamaguchi, Y., Suzuki, K., Yasuhara, M., Yamamoto, K., 2004. Quantum dots targeted to the assigned organelle in living cells. Microbiol. Immunol. 48, 985-94.

Howarth, M., Takao, K., Hayashi, Y., Ting, A.Y., 2005. Targeting quantum dots to surface proteins in living cells with biotin ligase. Proc. Natl. Acad. Sci. U S A 102, 7583-8.

Kim, S., Lim, Y.T., Soltesz, E.G., De Grand, A.M., Lee, J., Nakayama, A., Parker, J.A., Mihaljevic, T., Laurence, R.G., Dor, D.M. and others, 2004. Near-infrared fluorescent type II quantum dots for sentinel lymph node mapping. Nat. Biotechnol. 22, 93-7.

Lidke, D.S., Nagy, P., Heintzmann, R., Arndt-Jovin, D.J., Post, J.N., Grecco, H.E., Jares-Erijman, E.A., Jovin, T.M., 2004. Quantum dot ligands provide new insights into erbB/HER receptor-mediated signal transduction. Nat. Biotechnol. 22, 198-203.

Michalet, X., Pinaud, F.F., Bentolila, L.A., Tsay, J.M., Doose, S., Li, J.J., Sundaresan, G., Wu, A.M., Gambhir, S.S., Weiss, S., 2005. Quantum dots for live cells, in vivo imaging, and diagnostics. Science 307, 538-44.

Minamitani, H., Tsukada, K., Sekizuka, E., Oshio, C., 2003. Optical bioimaging: from living tissue to a single molecule: imaging and functional analysis of blood flow in organic microcirculation. J. Pharmacol. Sci. 93, 227-33.

Morgan, N.Y., English, S., Chen, W., Chernomordik, V., Russo, A., Smith, P.D., Gandjbakhche, A., 2005. Real time in vivo non-invasive optical imaging using near-infrared fluorescent quantum dots. Acad. Radiol. 12, 313-23.

Parungo, C.P., Colson, Y.L., Kim, S.W., Kim, S., Cohn, L.H., Bawendi, M.G., Frangioni, J.V., 2005. Sentinel lymph node mapping of the pleural space. Chest 127, 1799-804.

Ribatti, D., Nico, B., Bertossi, M., Roncali, L., Presta, M., 1997. Basic fibroblast growth factor-induced angiogenesis in the chick embryo chorioallantoic membrane: an electron microscopy study. Microvasc. Res. 53, 187-90.

Rickert, D., Moses, M.A., Lendlein, A., Kelch, S., Franke, R.P., 2003. The importance of angiogenesis in the interaction between polymeric biomaterials and surrounding tissue. Clin. Hemorheol. Microcirc. 28, 175-81.

Rieger, S., Kulkarni, R.P., Darcy, D., Fraser, S.E., Koster, R.W., 2005. Quantum dots are powerful multipurpose vital labeling agents in zebrafish embryos. Dev. Dyn. 234, 670-81.

Rizzo, V., DeFouw, D.O., 1996. Capillary sprouts restrict macromolecular extravasation during normal angiogenesis in the chick chorioallantoic membrane. Microvasc. Res. 52, 47-57.

Rizzo, V., Kim, D., Duran, W.N., DeFouw, D.O., 1995. Ontogeny of microvascular permeability to macromolecules in the chick chorioallantoic membrane during normal angiogenesis. Microvasc. Res. 49, 49-63.

Rizzo, V., Steinfeld, R., Kyriakides, C., DeFouw, D.O., 1993. The microvascular unit of the 6-day chick chorioallantoic membrane: a fluorescent confocal microscopic and ultrastructural morphometric analysis of endothelial permselectivity. Microvasc. Res. 46, 320-32.

Rosenthal, S.J., Tomlinson, I., Adkins, E.M., Schroeter, S., Adams, S., Swafford, L., McBride, J., Wang, Y., DeFelice, L.J., Blakely, R.D., 2002. Targeting cell surface receptors with ligand-conjugated nanocrystals. J. Am. Chem. Soc. 124, 4586-94.

Soltesz, E.G., Kim, S., Kim, S.W., Laurence, R.G., De Grand, A.M., Parungo, C.P., Cohn, L.H., Bawendi, M.G., Frangioni, J.V., 2006. Sentinel Lymph Node Mapping of the Gastrointestinal Tract by Using Invisible Light. Ann. Surg. Oncol.

Spanel-Borowski, K., 1989. The chick chorioallantoic membrane as test system for biocompatible materials. Res. Exp. Med. (Berl.) 189, 69-75.

Takatani, S., Graham, M.D., 1979. Theoretical analysis of diffuse reflectance from a two-layer tissue model. IEEE Trans. Biomed. Eng. 26, 656-64.

Tomlinson, I.D., Mason, J.N., Blakely, R.D., Rosenthal, S.J., 2005. Peptide-conjugated quantum dots: imaging the angiotensin type 1 receptor in living cells. Methods Mol. Biol. 303, 51-60.

Tozer, G.M., Ameer-Beg, S.M., Baker, J., Barber, P.R., Hill, S.A., Hodgkiss, R.J., Locke, R., Prise, V.E., Wilson, I., Vojnovic, B., 2005. Intravital imaging of tumour vascular networks using multi-photon fluorescence microscopy. Adv. Drug Deliv. Rev. 57, 135-52.

Valdes, T.I., Klueh, U., Kreutzer, D., Moussy, F., 2003. Ex ova chick chorioallantoic membrane as a novel in vivo model for testing biosensors. J. Biomed. Mater. Res. A 67, 215-23.

Valdes, T.I., Kreutzer, D., Moussy, F., 2002. The chick chorioallantoic membrane as a novel in vivo model for the testing of biomaterials. J. Biomed. Mater. Res. 62, 273-82.

Watson, A., Wu, X., Bruchez, M., 2003. Lighting up cells with quantum dots. Biotechniques 34, 296-300, 302-3.

Weidner, N., Semple, J.P., Welch, W.R., Folkman, J., 1991. Tumor angiogenesis and metastasis--correlation in invasive breast carcinoma. N. Engl. J. Med. 324, 1-8.

Wong, C., Inman, E., Spaethe, R., Helgerson, S., 2003. Fibrin-based biomaterials to deliver human growth factors. Thromb Haemost 89, 573-82.

Wu, X., Liu, H., Liu, J., Haley, K.N., Treadway, J.A., Larson, J.P., Ge, N., Peale, F., Bruchez, M.P., 2003. Immunofluorescent labeling of cancer marker Her2 and other cellular targets with semiconductor quantum dots. Nat. Biotechnol. 21, 41-6.

List of Figures

Figure 1: CAM vessel imaging using a range of emitting QDs. Individual QDs were injected into a CAM vein of 11-day old chicks and fluorescent images of CAM vasculature were obtained. A: Q565PEG-SAv, B: Q585PEG-SAv, C: Q605PEG-SAv, D: Q655AMP, E: Q705PEGa, F: Q755PEGa. Approximately 20 μL of a 2μM solution was injected for each QD. Image A was acquired with a Foveon HV-5M camera (MVIA, Inc.) with an AF Nikkor 50mm macro-lens (Nikon). Images B and C were taken using the Retiga EXia camera and M2BIO stereoscope (see Materials and Methods). Scale bars in all panels represent 1 mm.

Figure 2: Demonstration of QD versatility. QDs were injected into a CAM vein of 10-11-day old chick embryos. A: Whole-embryo fluorescence image using Q705PEGa. B: CAM vasculature and underlying yolk vessels imaged using Q755PEGa. C: Q705PEGa QDs were injected into an 11 day-old embryo. The following day a CAM vein and capillary structure were fluorescently imaged. QDs were no longer in vessel lumens but were endocytosed into the endothelial cells. A Fovean camera was used in A while a Retiga EXi camera was used in B and C. Magnifications: A, 1X; B, 1.6X Obj./1X zoom; C, 1.6X Obj./4X zoom. Scale bars in panels A, B, and C represent 25 mm, 1 mm, and 100 μm, respectively.

Figure 3: CAM vasculature imaged with QDs and FITC-Dextrans. A, B: Co-injected Q705PEGa (A) and 150kD FITC-Dextran (B) imaged just after injection. C, D: Co-injected Q705PEGa (C) and 40kD FITC-Dextran (D) imaged 1 hr post-injection. E, F: Co-injected Q705PEGa (E) and 40kD FITC-Dextran (F) imaged 3 hrs post-injection. G, H: Co-injected Q705PEGa (G) and 20kD FITC-Dextran imaged 15 minutes post-injection. Images were taken with a 1.6X objective and 1X zoom. Image acquisition times were 20 seconds for QD images and 60 seconds for FITC-Dextrans. Scale bars in all panels represent 1 mm.

Figure 4: CAM vessel fluorescence followed over time for Q705PEGa and 500kD FITC-Dextran. 500kD FITC-Dextran (A-D) and Q705PEGa (E-H) were co-injected and images were taken at the designated times. Imaging details were the same as in Figure 1. Scale bars in all panels represent 1 mm.

Figure 5: Capillaries imaged by QDs and FITC-Dextrans. Q705PEGa (A) and 150kD FITC-Dextran (B) were co-injected in a chick CAM and capillary images were taken just after injection. Q705PEGa (C) and 500kD FITC-Dextran (D) were co-injected in a chick CAM and capillary images were taken just after injection. Images were acquired using a 10X objective and 4X zoom. Image acquisition times were 1 second for QDs and 3 seconds for FITC-Dextrans. Scale bars in all panels represent 250 μm.

Figure 6. CAM angiogenic responses to fibrin-based constructs containing FGF-2 imaged using QDs and FITC-Dextrans. After bFGF containing fibrin-based constructs were on the chick CAM for 2 days QDs and FITC-Dextrans were co-injected and fluorescence images were taken just after injection. A-D: Angiogenic responses

comparing 150kD FITC-Dextran (A, C) to Q705PEGa (B, D). E-H: Angiogenic responses comparing 500kD FITC-Dextran (E, G) to Q705PEGa (F) and Q800PEGm (H). Images were taken with a 1.6X objective and a 1X zoom. Image acquisition times were 10 seconds for QDs and 30 seconds for FITC-Dextrans. Scale bars represent 2 mm.

Figure 7. QDs retain fluorescence after exposure to fixatives. Fibrin gels containing 605PEG-SAv (A), 655PEG-SAv (B), or 705PEG-SAv QDs (C) were fixed with 1% paraformaldehyde or 1% glutaraldehyde for 30 minutes followed by three 5 min washes with PBS. Initial (I) and glutaraldehyde (G) or paraformaldehyde (P) treated control and QD-containing gel fluorescence intensities were measured using Image J software. Fluorescence intensities for 605PEG-SAv glutaraldehyde treated gels were corrected for the autofluorescence induced by glutaraldehyde treatment of the control (G*). Data is reported as the average of 3 samples +/- the standard deviation.

Figure 8. QDs survive paraffin histological processing. Fibrin gels containing bFGF and fibrin-bound 605PEG-SAv QDs were placed on the CAM of 10-day old chick embryos. Approximately 48 hours later 705PEGa QDs were injected into a CAM vein and the fibrin and surrounding CAM were excised and fixed in 1% paraformaldehyde overnight at 4°C. Samples were processed for embedding in paraffin and sectioned at 5 μm thickness. The interfacial area between the invading CAM and fibrin construct is shown. A: Fibrin-bound 605PEG-SAv QD fluorescence demonstrates fibrin degradation and remodeling by the invading CAM. B: Blood vessel-labeled 705PEGa QD fluorescence shows blood vessels primarily oriented perpendicular to the CAM/fibrin interface. Arrows indicate vessel lumens oriented perpendicular to the image plane.

Figure 9. QDs identified within transmission electron micrographs. Three days post-placement of fibrin gels containing bFGF on the CAM, 705PEGa QDs were injected into CAM veins followed by excision, fixation, and TEM processing as described in the Materials and Methods. Endothelial cells (EC) lining a vessel lumen are shown: the insert shows a vesicle containing endocytosed QDs.

Table 1

FITC-Dextran and QD vascular half-life measurements.[1]

Molecule	Half-life (hours)	Sample Size (n)	Concentration Tested
Q705PEGa	11.0 ± 0.7	10	3.5 μM
Q705AMP	4.9 ± 0.1	5	3.5 μM
500 kD FITC-Dextran	10.3 ± 1.3	5	98 μM
150 kD FITC-Dextran	8.9 ± 0.7	5	357 μM
70 kD FITC-Dextran	6.0 ± 0.3	2	850 μM
40 kD FITC-Dextran	0.25	1	1200 μM
20 kD FITC-Dextran	0.08 ± 0.0	2	2860 μM

[1]Half-lives are reported as the mean +/- SEM

Figure 1

Click here to download high resolution image

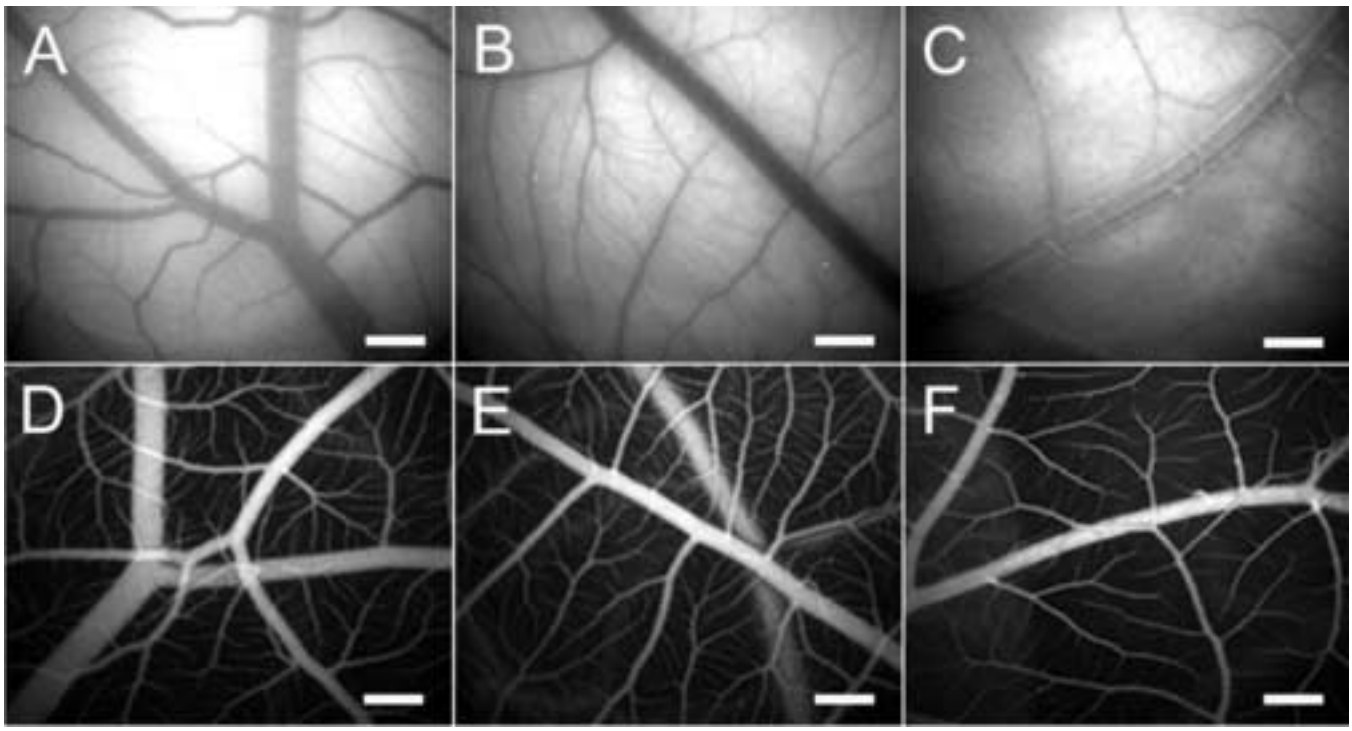

Figure 2

Click here to download high resolution image

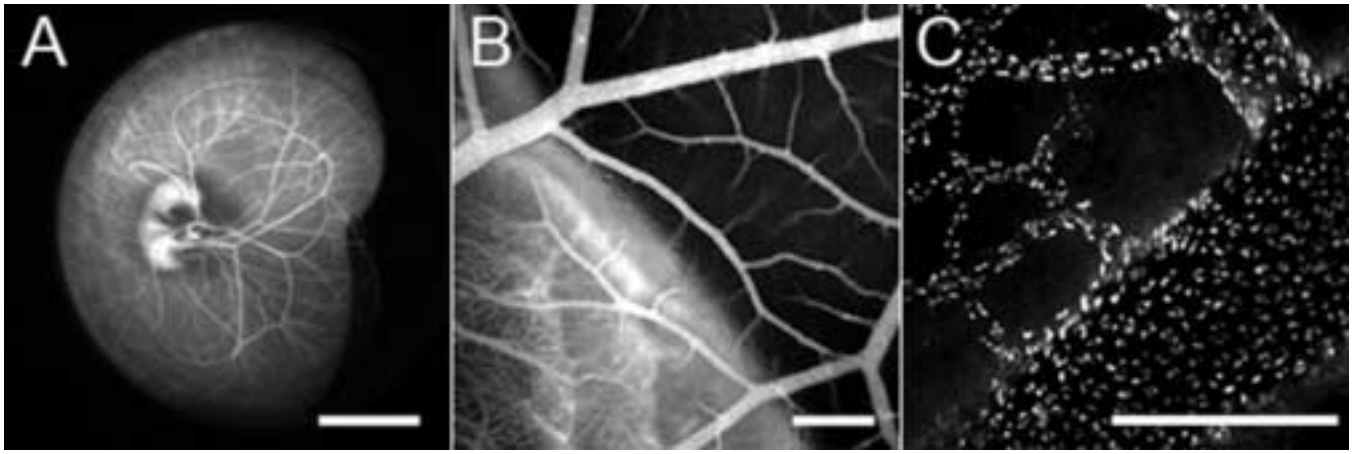

Figure 3

Click here to download high resolution image

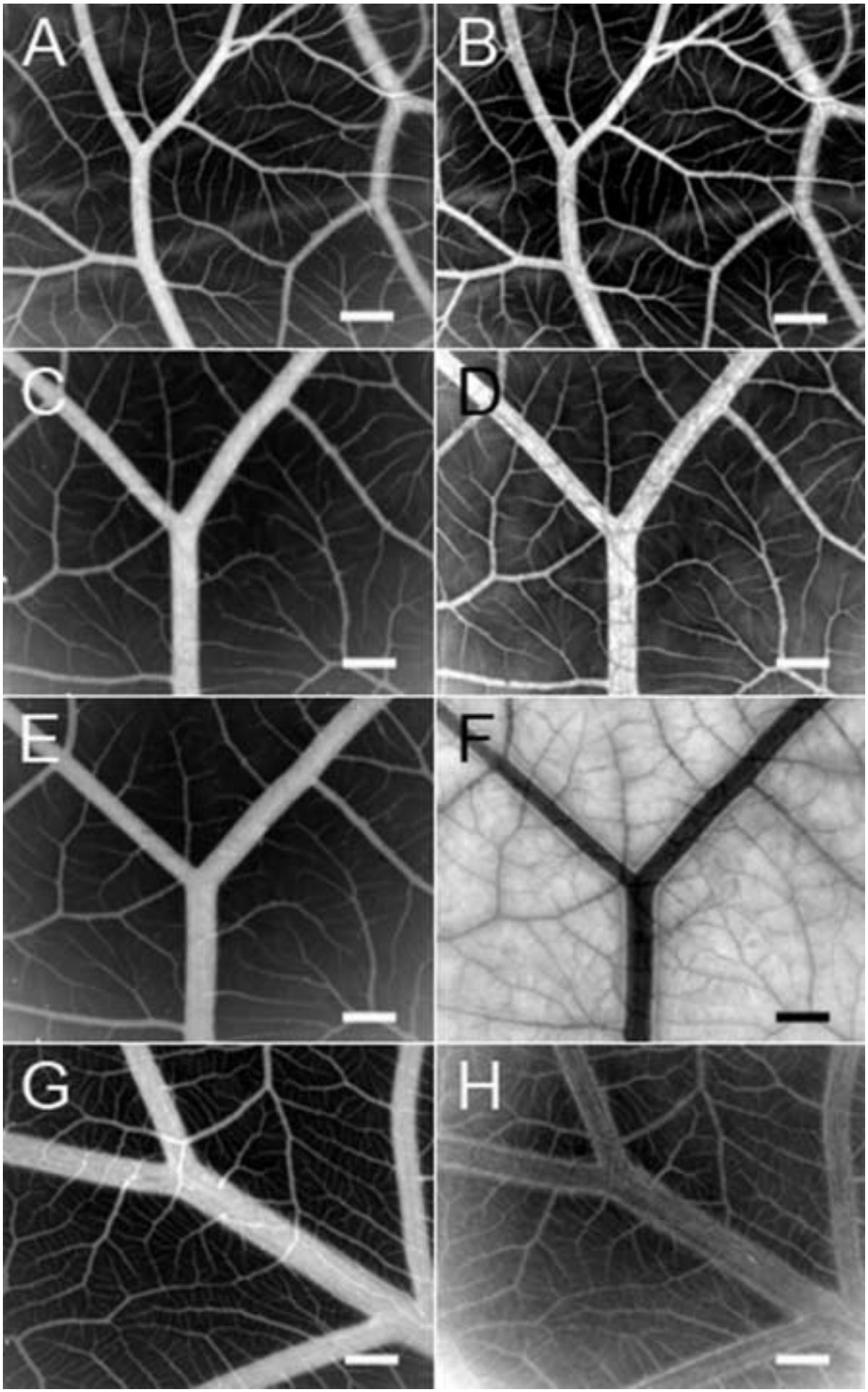

Figure 4

Click here to download high resolution image

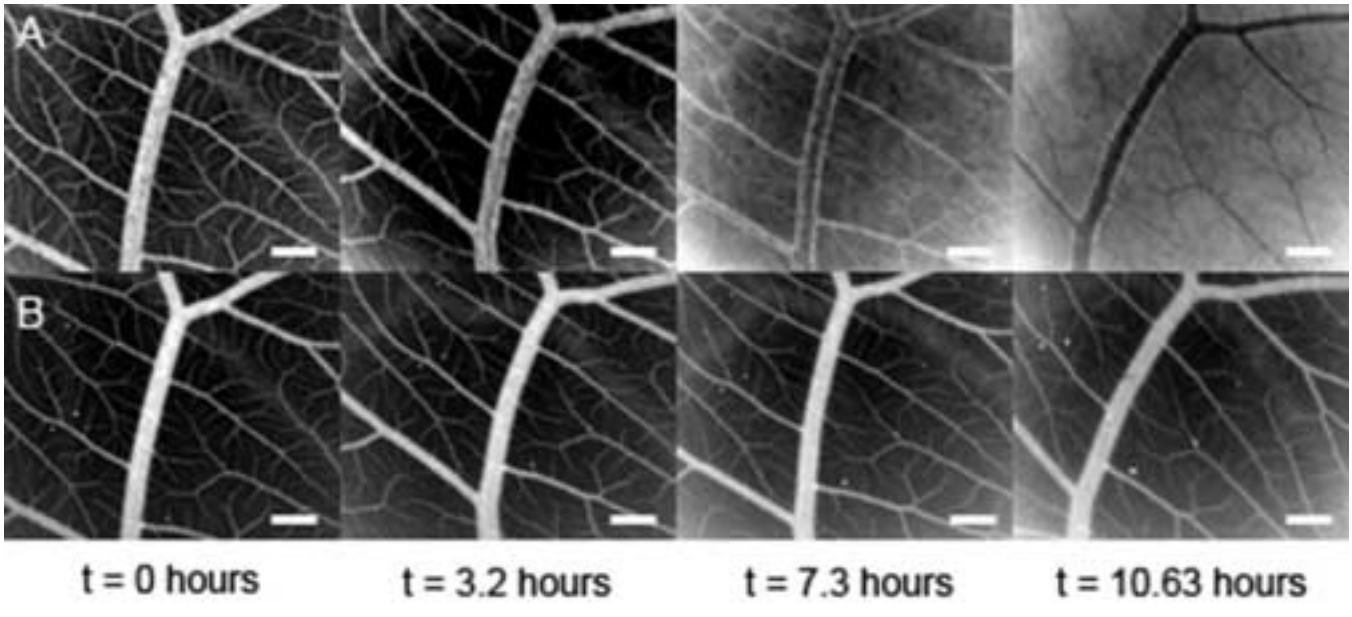

Figure 5

Click here to download high resolution image

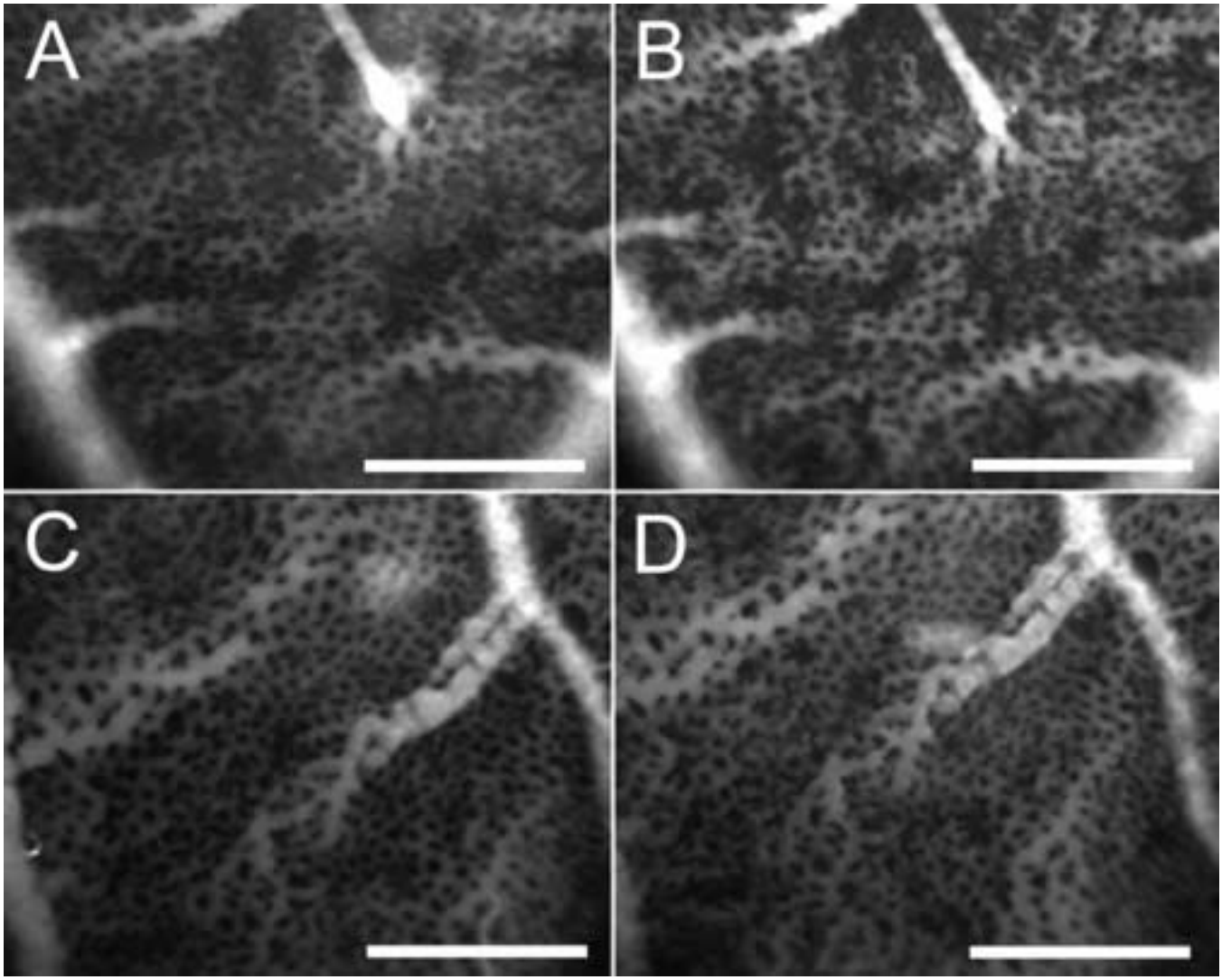

Figure 6

Click here to download high resolution image

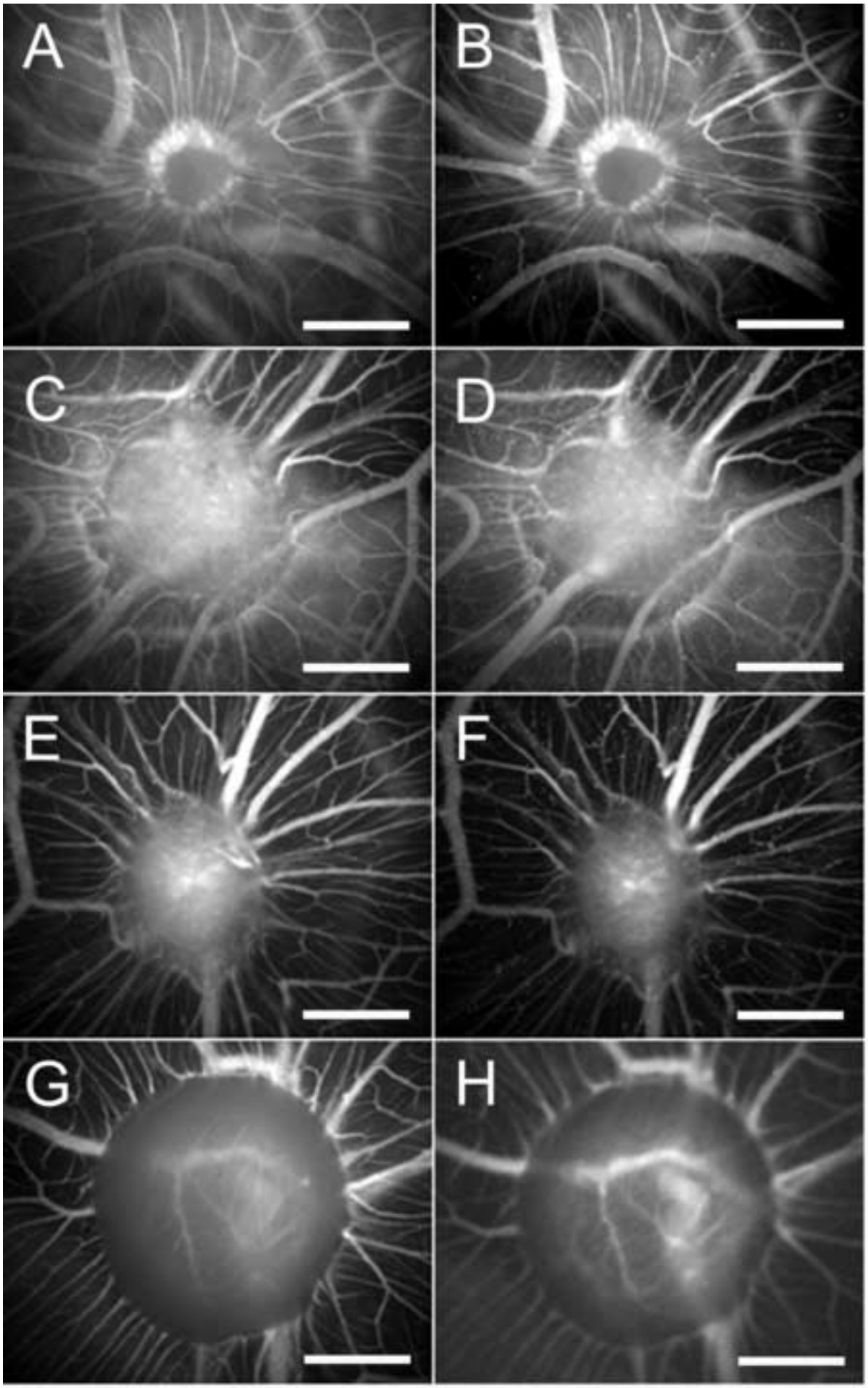

Figure 7

Click here to download high resolution image

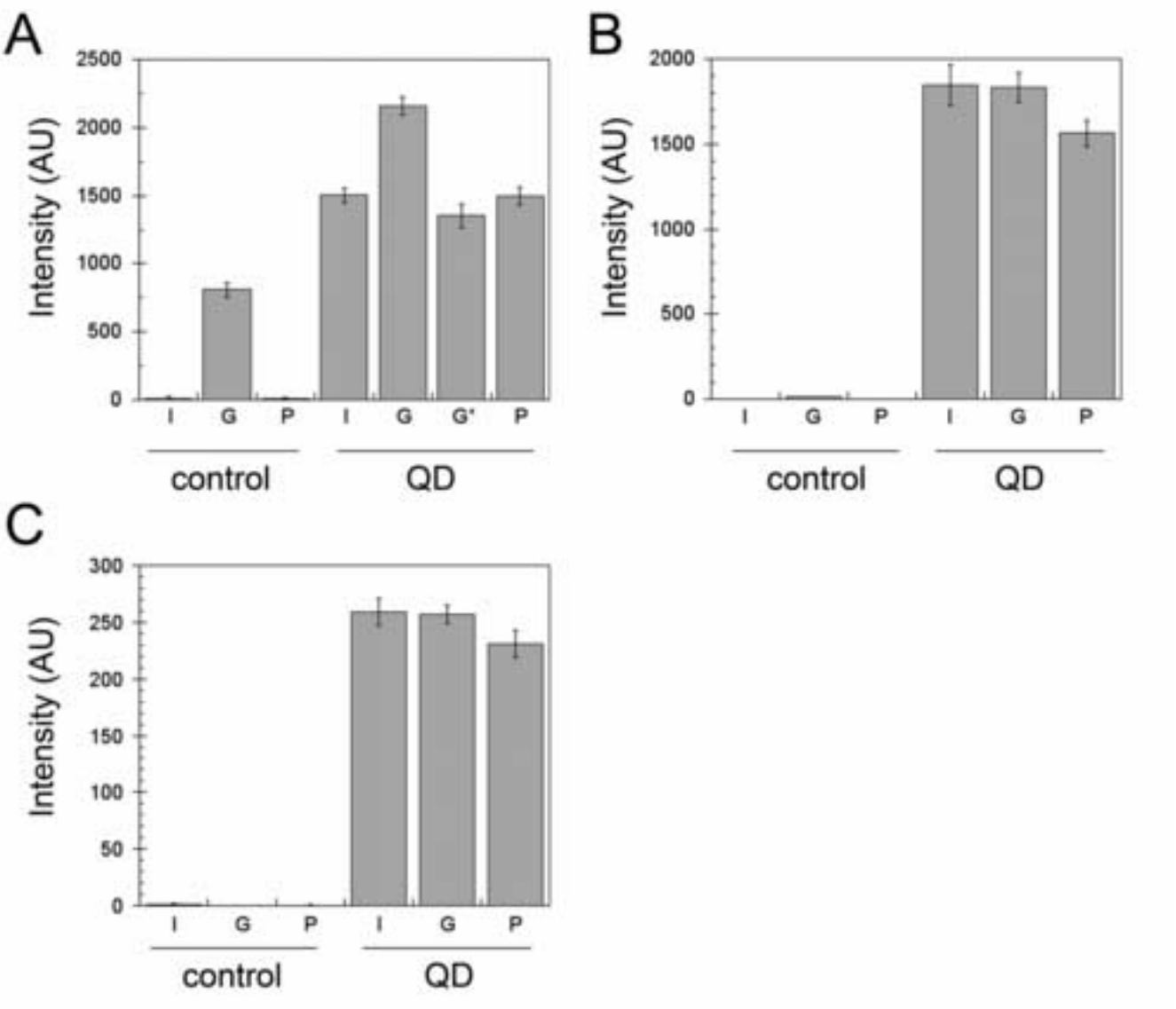

Figure 8

Click here to download high resolution image

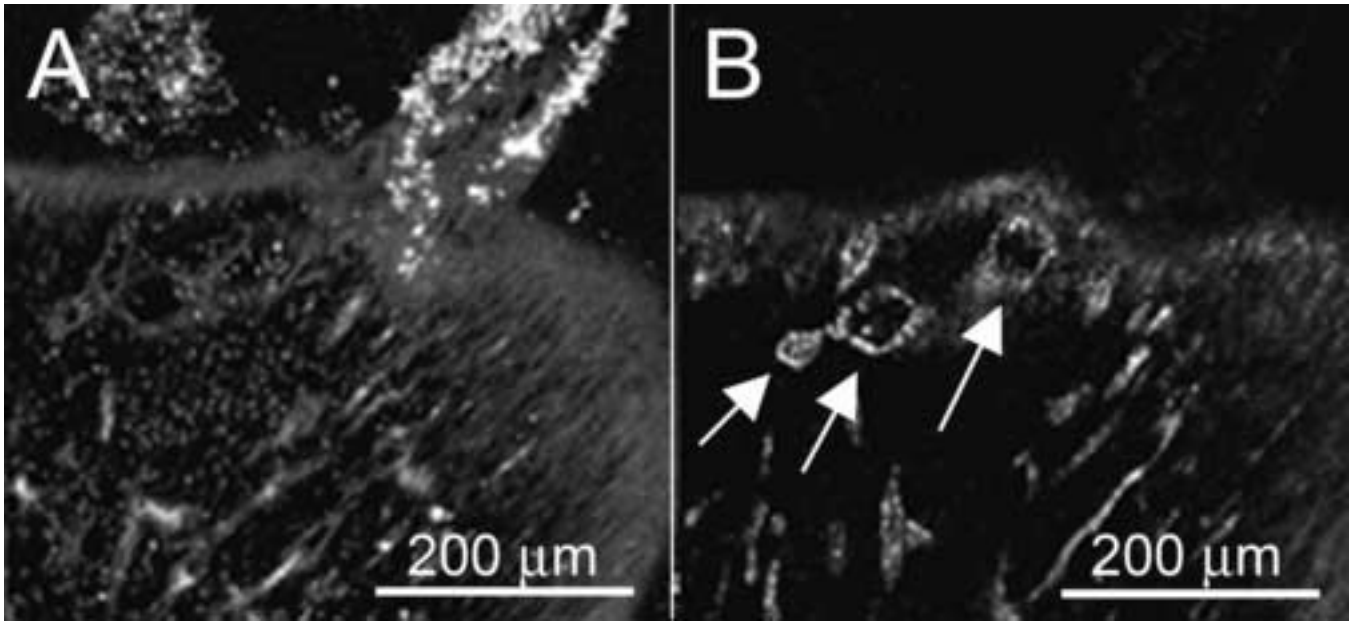

Figure 9

Click here to download high resolution image